





Cortical neurodegeneration caused by *Psen1* mutations is independent of A β

Kuo Yan^{a,1}, Chen Zhang^a, Jongkyun Kang^a, Paola Montenegro^a , and Jie Shen^{a,b,2} 

Affiliations are included on p. 8.

Edited by Lawrence Goldstein, University of California at San Diego, La Jolla, CA; received June 16, 2024; accepted July 16, 2024

Mutations in the *PSEN* genes are the major cause of familial Alzheimer's disease, and presenilin (PS) is the catalytic subunit of γ -secretase, which cleaves type I transmembrane proteins, including the amyloid precursor protein (APP) to release A β peptides. While PS plays an essential role in the protection of neuronal survival, *PSEN* mutations also increase the ratio of A β ₄₂/A β ₄₀. Thus, it remains unresolved whether *PSEN* mutations cause AD via a loss of its essential function or increases of A β ₄₂/A β ₄₀. Here, we test whether the knockin (KI) allele of *Psen1* L435F, the most severe FAD mutation located closest to the active site of γ -secretase, causes age-dependent cortical neurodegeneration independent of A β by crossing various *Psen* mutant mice to the *App*-null background. We report that removing A β completely through APP deficiency has no impact on the age-dependent neurodegeneration in *Psen* mutant mice, as shown by the absence of effects on the reduced cortical volume and decreases of cortical neurons at the ages of 12 and 18 mo. The L435F KI allele increases A β ₄₂/A β ₄₀ in the cerebral cortex while decreasing de novo production and steady-state levels of A β ₄₂ and A β ₄₀ in the presence of APP. Furthermore, APP deficiency does not alleviate elevated apoptotic cell death in the cerebral cortex of *Psen* mutant mice at the ages of 2, 12, and 18 mo, nor does it affect the progressive microgliosis in these mice. Our findings demonstrate that *Psen1* mutations cause age-dependent neurodegeneration independent of A β , providing further support for a loss-of-function pathogenic mechanism underlying *PSEN* mutations.

Alzheimer's disease | Presenilin | APP | apoptosis | gliosis

Mutations in the *Presenilin* (*PSEN1* and *PSEN2*) genes are the major cause of familial Alzheimer's disease (FAD) (1, 2). Presenilin (PS) constitutes the catalytic subunit of γ -secretase, a multisubunit intramembrane aspartate protease that cleaves type I transmembrane proteins including the amyloid precursor protein (APP) and Notch (3–5). Mutations in the *APP* gene are also linked to FAD, and β -amyloid (A β) peptides released by γ -secretase are a major component of extracellular amyloid plaques observed in AD brains (6). The initial report of the increased ratio of A β ₄₂/A β ₄₀ in transgenic mice overexpressing *PSEN1* mutations (7), along with similar increases of A β ₄₂/A β ₄₀ in FAD patients (8), suggested that *PSEN* mutations might cause FAD via a toxic gain-of-function mechanism, providing key evidence for the amyloid hypothesis (9). Hence, removal of A β by inhibition of γ -secretase or anti-A β antibodies became the major therapeutic efforts by pharmaceutical companies to treat AD.

The large number (>450) of mostly missense mutations found in the *PSEN1* and *PSEN2* genes scattering throughout the coding sequences, however, is also consistent with a partial loss-of-function pathogenic mechanism. Distinguishing between these two possibilities thereby is critically important for AD therapeutics. The development of *Psen* conditional double knockout (cDKO) mice demonstrated that selective PS inactivation in excitatory or inhibitory neurons results in memory and synaptic impairments followed by striking age-dependent neurodegeneration in the cerebral cortex (10–22), raising the possibility that *PSEN* mutations may cause FAD via a loss-of-function mechanism (23). Moreover, cell culture studies showed that *PSEN* mutations cause loss of γ -secretase activity (24, 25), and the most severe FAD *PSEN1* mutations, such as L435F and C410Y, genocopy *Psen1*-null mice and result in undetectable γ -secretase activity in homozygous knockin (KI) mice (26, 27). The L435F KI allele also causes memory and synaptic impairment as well as age-dependent neurodegeneration (26, 28). Subsequent biochemical studies of 138 distinct *PSEN1* mutations showed that ~90% of mutations lead to impaired γ -secretase activity, whereas 30% of mutations abolish its activity (29, 30), and human neurons derived from isogenic iPSCs carrying either *PSEN1* exon 9 deletion or wild-type allele

Significance

Alzheimer's disease (AD) is the most common neurodegenerative disorder. During the last two decades, substantial efforts from pharmaceutical companies have targeted amyloid peptides as disease-modifying therapies. The elevated A β ₄₂/A β ₄₀ ratio in familial AD patients carrying *PSEN* mutations has been taken as crucial evidence for a causal role of A β in the pathogenesis. The current genetic study using APP deficiency to remove A β completely in various *Psen* mutant mice provides compelling experimental evidence for the lack of a causal role of A β in the age-dependent neurodegeneration and elevated apoptotic cell death in the cerebral cortex caused by *Psen* mutations. These findings suggest that removal of A β is unlikely to be effective for treating familial AD patients carrying *PSEN* mutations.

Competing interest statement: J.S. was a co-founder and scientific advisor of Paros Bio and iNeuro Therapeutics and received consulting fees. J.S.'s interests have been managed by Mass General Brigham in accordance with the institutional conflict of interest policies. J.S. owns stocks of iNeuro Therapeutics, a private company.

This article is a PNAS Direct Submission.

Copyright © 2024 the Author(s). Published by PNAS. This open access article is distributed under Creative Commons Attribution-NonCommercial-NoDerivatives License 4.0 (CC BY-NC-ND).

¹Present address: Institute of Cell Biology and Neurobiology, Charité–Universitätsmedizin Berlin, 10117 Berlin, Germany.

²To whom correspondence may be addressed. Email: jshen@bwh.harvard.edu.

This article contains supporting information online at <https://www.pnas.org/lookup/suppl/doi:10.1073/pnas.2409343121/-DCSupplemental>.

Published August 13, 2024.

also showed decreased γ -secretase activity by the *PSEN1* $\Delta E9$ allele (31). These findings demonstrate not only essential functions of PS in the key processes relevant to AD pathogenesis but also impairment of γ -secretase and physiological roles of PS by FAD *PSEN* mutations.

However, it remains unresolved whether *PSEN* mutations cause AD via the loss of its essential function or increases of A β 42/A β 40. While γ -secretase activity and generation of A β are undetectable in homozygous L435F and C410F KI brains, A β 42/A β 40 is elevated in heterozygous L435F KI brains. Thus, it is possible that the increase in A β 42/A β 40 may drive age-dependent cortical neurodegeneration observed in these *Psen* mutant mice (26, 27). It was also reported that L435F and C410Y mutations generated very high levels of A β 43 in immortalized cell lines overexpressing mutant APP, which might provide amyloidogenic A β seeds that trigger neurodegeneration (32). Here, we test whether the KI allele of *Psen1* L435F, the most severe FAD mutation located closest to the active site of γ -secretase, causes age-dependent cortical neurodegeneration independent of A β by crossing various *Psen* mutant mice to the *App*-null background, which removes all A β species completely. Surprisingly, despite the increase of A β 42/A β 40 by the L435F KI allele in the presence of APP and the elimination of A β in the absence of APP, APP deficiency has no impact on the age-dependent reduction of cortical volume and decreases of cortical neurons caused by the L435F KI allele at the ages of 12 and 18 mo. Furthermore, APP deficiency does not rescue elevated apoptotic cell death in the cerebral cortex of *Psen* mutant mice at the ages of 2, 12, and 18 mo, nor does it affect the progressive microgliosis in *Psen* mutant mice. Taken together, these findings demonstrate that *Psen* mutations cause age-dependent neurodegeneration independent of A β , providing further experimental support for the presenilin hypothesis.

Results

APP Deficiency Has No Effect on Neurodegeneration Caused by *Psen1* Mutations. We previously reported that the *Psen1* L435F KI allele results in age-dependent neurodegeneration, as shown by the progressive reduction of cortical volume and neuron number at 12 and 18 mo of age (26). While the production of A β 40, A β 42, and A β 43 is decreased in KI brains in a KI allele-dependent manner, A β 42/A β 40 is increased in the cerebral cortex of heterozygous KI mice, which raises the possibility that elevated A β 42/A β 40 may contribute to the cortical neurodegeneration caused by the *Psen1* L435F KI allele (26, 27). Furthermore, another study using immortalized cell lines overexpressing mutant *App* and *Psen1* L435F reported extremely high levels of A β 43, which suggested that seeded amyloid aggregation might have contributed to the observed neurodegeneration in L435F KI mice (27, 32). To determine whether the relative increase of the more amyloidogenic A β 42 and A β 43 contributes to the observed age-dependent neurodegeneration in *Psen* mutant mice, we use *App*-null alleles to remove all A β species genetically. We compare the effects of the *Psen1* L435F KI allele, relative to the *Psen1* wild-type allele and *Psen1* conditional null allele, on cortical neuronal survival in the presence of APP (four *Psen* genotypic groups) or in the absence of APP (four corresponding genotypic groups in the *App*-null background), and all eight genotypic groups were essentially "littermates" obtained from a large set of breeding pairs to ensure their similar genetic background, as each genotype was obtained in the ratio of 1/16. The floxed *Psen1* alleles in *Psen1*^{F/F} mice, in which the two loxP sites were introduced into *Psen1* introns 1 and 3, were confirmed previously for the absence of the effects on transcription, splicing, and translation of the *Psen1*

gene, representing the wild-type *Psen1* gene (16). Relative to the wild-type *Psen1* allele, the *Psen1* L435F KI allele causes age-dependent neurodegeneration at the ages of 12 and 18 mo in *Psen1*^{KI/F}; *Psen2*^{-/-}; *Cre* mice, compared with *Psen1*^{KI/+}; *Psen2*^{-/-}; *Cre* mice, indicating that one copy of the *Psen1* gene is sufficient to support cortical neuron survival in mice (26).

To determine whether APP deficiency affects neurodegeneration caused by the L435F KI allele, we performed quantitative histological analysis of all eight genotypic groups at the ages of 2, 12, and 18 mo. For simplicity and clarity, we present the data obtained from four genotypic groups carrying the L435F KI allele in Fig. 1, whereas the results from all eight genotypic groups are included in *SI Appendix*, Fig. S1. Nissl and NeuN staining revealed no gross abnormality in the cerebral cortex of any of the eight genotypic groups at 2 mo of age (Fig. 1 *A* and *C* and *SI Appendix*, Fig. S1 *A* and *C*). Using stereological methods, we quantified the volume of the neocortex and the number of NeuN+ neurons in the neocortex and found similar cortical volume and neuron number in all eight genotypic groups (Fig. 1*B* and *SI Appendix*, Fig. S1*B*).

At 12 mo of age, *Psen1*^{KI/F}; *Psen2*^{-/-}; *Cre* mice show a significant reduction (-23%) in cortical volume (24.47 ± 0.30 mm³), relative to *Psen1*^{KI/F}; *Psen2*^{-/-} (31.60 ± 0.47 mm³, $P < 0.0001$) and *Psen1*^{F/F}; *Psen2*^{-/-} mice (31.57 ± 0.67 mm³, $P < 0.0001$, two-way ANOVA with Tukey's post hoc comparisons; Fig. 1*B* and *SI Appendix*, Fig. S1*B*). However, the cortical volume in *Psen1*^{KI/F}; *Psen2*^{-/-}; *Cre* mice (24.47 ± 0.30 mm³) is similar to those in *Psen1*^{KI/F}; *Psen2*^{-/-}; *Cre*; *App*^{-/-} mice (23.67 ± 0.48 mm³, $P > 0.99$; Fig. 1*B*), indicating that removal of APP or A β does not affect the reduction of cortical volume in these mutant mice. APP deficiency also does not affect the decrease of cortical volume observed in *Psen* cDKO mice (20.00 ± 0.33 mm³), compared with *Psen* cDKO; *App*^{-/-} mice (19.72 ± 0.38 mm³, $P > 0.99$; *SI Appendix*, Fig. S1*B*). Furthermore, the neuron number in the neocortex is also significantly reduced (-16%) in *Psen1*^{KI/F}; *Psen2*^{-/-}; *Cre* mice ($3.87 \pm 0.05 \times 10^6$), relative to *Psen1*^{KI/F}; *Psen2*^{-/-} mice ($4.61 \pm 0.03 \times 10^6$, $P < 0.0001$) and *Psen1*^{F/F}; *Psen2*^{-/-} ($4.65 \pm 0.05 \times 10^6$, $P < 0.0001$). The neuron number in the neocortex of *Psen1*^{KI/F}; *Psen2*^{-/-}; *Cre* ($3.87 \pm 0.05 \times 10^6$) is nearly identical to those in *Psen1*^{KI/F}; *Psen2*^{-/-}; *Cre*; *App*^{-/-} mice ($3.85 \pm 0.09 \times 10^6$, $P > 0.99$), indicating further that APP deficiency does not rescue the loss of cortical neurons in these *Psen* mutant mice (Fig. 1*D*). Similarly, the cortical neuron number ($P > 0.99$) is similar between *Psen* cDKO and *Psen* cDKO; *App*^{-/-} mice (*SI Appendix*, Fig. S1*D*).

By 18 mo of age, *Psen1*^{KI/F}; *Psen2*^{-/-}; *Cre* mice show a further reduction (-32%) of cortical volume (20.99 ± 0.31 mm³), relative to *Psen1*^{KI/F}; *Psen2*^{-/-} (30.66 ± 0.42 mm³, $P < 0.0001$) and *Psen1*^{F/F}; *Psen2*^{-/-} (30.92 ± 0.38 mm³, $P < 0.0001$; Fig. 1*B* and *SI Appendix*, Fig. S1*B*). However, the volume of the neocortex in *Psen1*^{KI/F}; *Psen2*^{-/-}; *Cre* mice (20.99 ± 0.31 mm³) is similar to that in *Psen1*^{KI/F}; *Psen2*^{-/-}; *Cre*; *App*^{-/-} mice (20.59 ± 0.52 mm³, $P > 0.99$). Furthermore, the number of cortical neurons in *Psen1*^{KI/F}; *Psen2*^{-/-}; *Cre* mice ($3.43 \pm 0.05 \times 10^6$) is also reduced (-25%), relative to *Psen1*^{KI/F}; *Psen2*^{-/-} ($4.55 \pm 0.04 \times 10^6$, $P < 0.0001$) and *Psen1*^{F/F}; *Psen2*^{-/-} mice ($4.50 \pm 0.05 \times 10^6$, $P < 0.0001$), but is similar to those in *Psen1*^{KI/F}; *Psen2*^{-/-}; *Cre*; *App*^{-/-} mice ($3.38 \pm 0.08 \times 10^6$, $P > 0.99$; Fig. 1*D* and *SI Appendix*, Fig. S1*D*). The reduction of cortical volume (-49%) and neuron number (-38%) in *Psen* cDKO mice is greater compared to *Psen1*^{KI/F}; *Psen2*^{-/-}; *Cre* mice, suggesting that the *Psen1* L435F KI allele retains some protection to neuronal survival relative to the *Psen1* conditional null allele (*SI Appendix*, Fig. S1). Nevertheless, cortical neuron number is essentially the same ($P > 0.99$) between *Psen* cDKO ($2.77 \pm 0.08 \times 10^6$) and *Psen* cDKO; *App*^{-/-} mice ($2.82 \pm 0.01 \times 10^6$; *SI Appendix*, Fig. S1*D*). Furthermore, our analysis of *App*^{-/-} mice at the ages of 2, 12, and

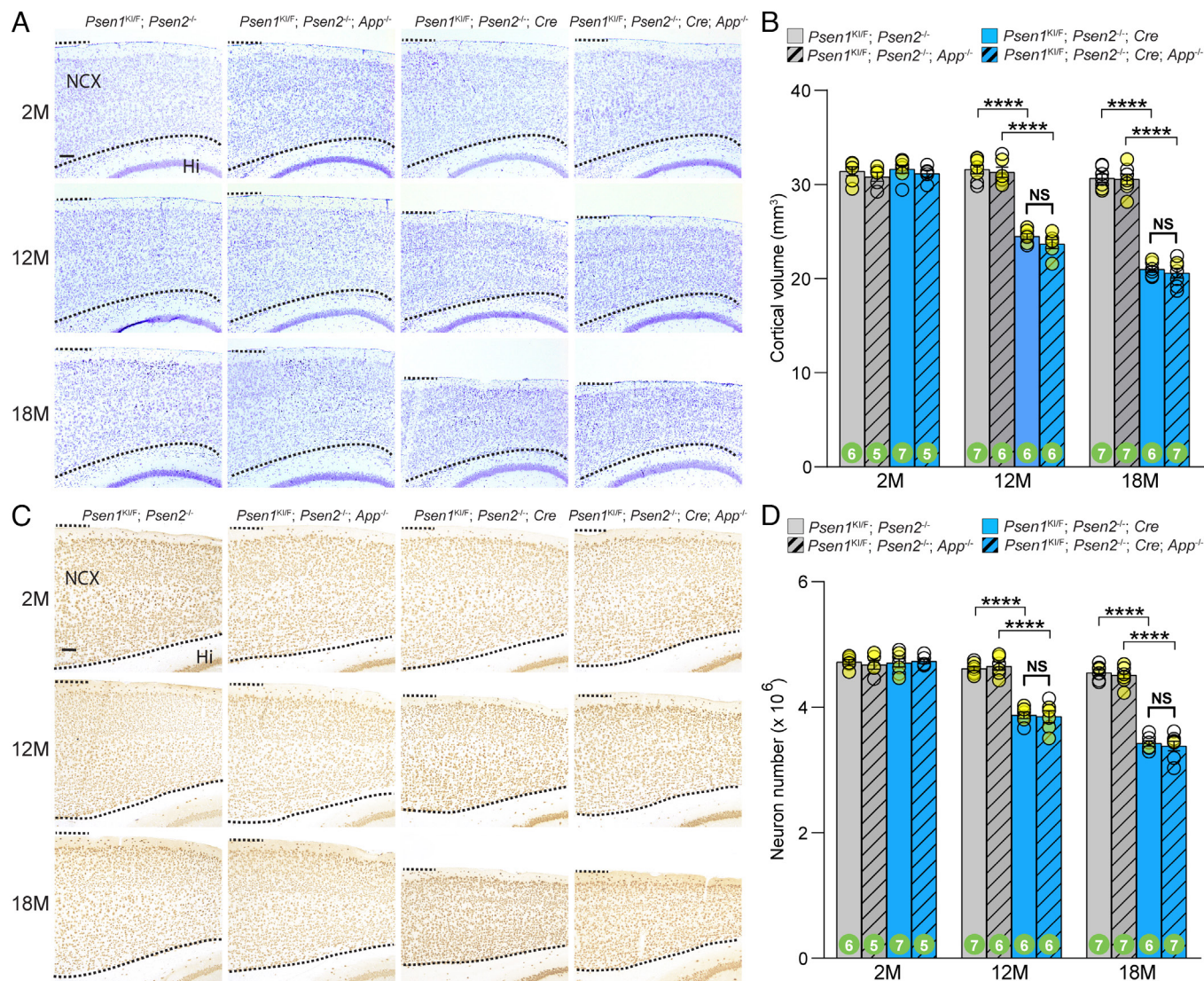


Fig. 1. APP deficiency does not affect neurodegeneration caused by *Psen1* mutations. (A) Nissl staining of comparable sagittal sections of *Psen1^{Kl/F}; Psen2^{-/-}; Cre*, *Psen1^{Kl/F}; Psen2^{-/-}; Cre; App^{-/-}*, and littermate controls at the ages of 2, 12, and 18 mo. (Scale bar, 100 μ m.) (B) Stereological quantification shows genotype-specific, age-dependent reductions of cortical volume ($F_{4,67} = 61.91$, $P < 0.0001$, two-way ANOVA). At 2 mo of age, all four genotypic groups have similar cortical volume ($P > 0.99$; two-way ANOVA with Tukey's post hoc comparisons). At 12 mo of age, the volume of the neocortex in *Psen1^{Kl/F}; Psen2^{-/-}; Cre* mice (24.47 ± 0.30 mm³) is significantly reduced ($\sim 23\%$), relative to *Psen1^{Kl/F}; Psen2^{-/-}* mice (31.60 ± 0.47 mm³; $P < 0.0001$). However, the cortical volume is similar between *Psen1^{Kl/F}; Psen2^{-/-}; Cre* mice (24.47 ± 0.30 mm³) and *Psen1^{Kl/F}; Psen2^{-/-}; Cre; App^{-/-}* mice (23.67 ± 0.48 mm³; $P > 0.99$). At 18 mo of age, the cortical volume in *Psen1^{Kl/F}; Psen2^{-/-}; Cre* mice (20.99 ± 0.31 mm³) is lower ($\sim 32\%$) than that in *Psen1^{Kl/F}; Psen2^{-/-}* mice (30.66 ± 0.42 mm³; $P < 0.0001$). However, the cortical volume is essentially identical between *Psen1^{Kl/F}; Psen2^{-/-}; Cre* mice (20.99 ± 0.31 mm³) and *Psen1^{Kl/F}; Psen2^{-/-}; Cre; App^{-/-}* mice (20.59 ± 0.52 mm³; $P > 0.99$). (C) NeuN staining of comparable sagittal sections of all four genotypic groups at the ages of 2, 12, and 18 mo. (Scale bar, 100 μ m.) (D) Stereological quantification shows genotype-specific, age-dependent reductions of neurons in the neocortex ($P > 0.99$). At 12 mo of age, the number of neurons in the neocortex of *Psen1^{Kl/F}; Psen2^{-/-}; Cre* ($3.87 \pm 0.05 \times 10^6$) mice is significantly reduced ($\sim 16\%$), relative to *Psen1^{Kl/F}; Psen2^{-/-}* mice ($4.61 \pm 0.03 \times 10^6$; $P < 0.0001$). However, the number of neurons in the neocortex is essentially identical between *Psen1^{Kl/F}; Psen2^{-/-}; Cre* mice ($3.87 \pm 0.05 \times 10^6$) and *Psen1^{Kl/F}; Psen2^{-/-}; Cre; App^{-/-}* mice ($3.85 \pm 0.09 \times 10^6$; $P > 0.99$). By 18 mo of age, the number of neurons in the neocortex is further reduced ($\sim 25\%$) in *Psen1^{Kl/F}; Psen2^{-/-}; Cre* mice ($3.43 \pm 0.05 \times 10^6$), relative to *Psen1^{Kl/F}; Psen2^{-/-}* mice ($4.55 \pm 0.04 \times 10^6$; $P < 0.0001$), but the cortical neuron number is nearly identical between *Psen1^{Kl/F}; Psen2^{-/-}; Cre* ($3.43 \pm 0.05 \times 10^6$) and *Psen1^{Kl/F}; Psen2^{-/-}; Cre; App^{-/-}* mice ($3.38 \pm 0.08 \times 10^6$; $P > 0.99$). All data represent mean \pm SEM. **** $P < 0.0001$. NS, not significant. The value in the column indicates the number of mice used in each experiment. Yellow-filled and open circles represent data obtained from individual male and female mice, respectively.

18 mo showed that *App^{-/-}* mice do not develop age-dependent loss of cortical volume or decreases of cortical neurons (SI Appendix, Fig. S2).

Increased A β 42/A β 40 but Reduced A β Levels by Heterozygous L435F KI Alleles. We previously reported that steady-state levels of endogenous A β 40 and A β 42 are reduced in the cortex of L435F *Psen1^{Kl/F}* mice, though the ratio of A β 42/A β 40 is elevated, which is sufficient to accelerate amyloid deposition of human A β derived from an overexpressed human mutant APP transgene (26). We therefore similarly used ELISA to measure steady-state levels of

endogenous A β 40 and A β 42 in the cortex of all genotypic groups at the ages of 2 and 12 mo (Fig. 2). Consistent with the prior report (26), we found significantly decreased levels A β 40 in the soluble (0.31 ± 0.02 ; $F_{5,22} = 322.20$, $P < 0.0001$, one-way ANOVA with Tukey's post hoc comparisons) and insoluble (0.44 ± 0.02 ; $P < 0.0001$) fractions derived from the cortex of *Psen1^{Kl/F}; Psen2^{-/-}* mice at 2 mo of age, relative to *Psen1^{F/F}; Psen2^{-/-}* mice (soluble: 0.38 ± 0.01 ; $P < 0.0001$, insoluble: 0.61 ± 0.02 ; $P < 0.0001$), and levels of A β 40 are more dramatically reduced in *Psen1^{Kl/F}; Psen2^{-/-}; Cre* mice (soluble: 0.10 ± 0.003 , $P < 0.0001$; insoluble: 0.19 ± 0.01 ; $P < 0.0001$), compared to *Psen1^{Kl/F}; Psen2^{-/-}* mice.

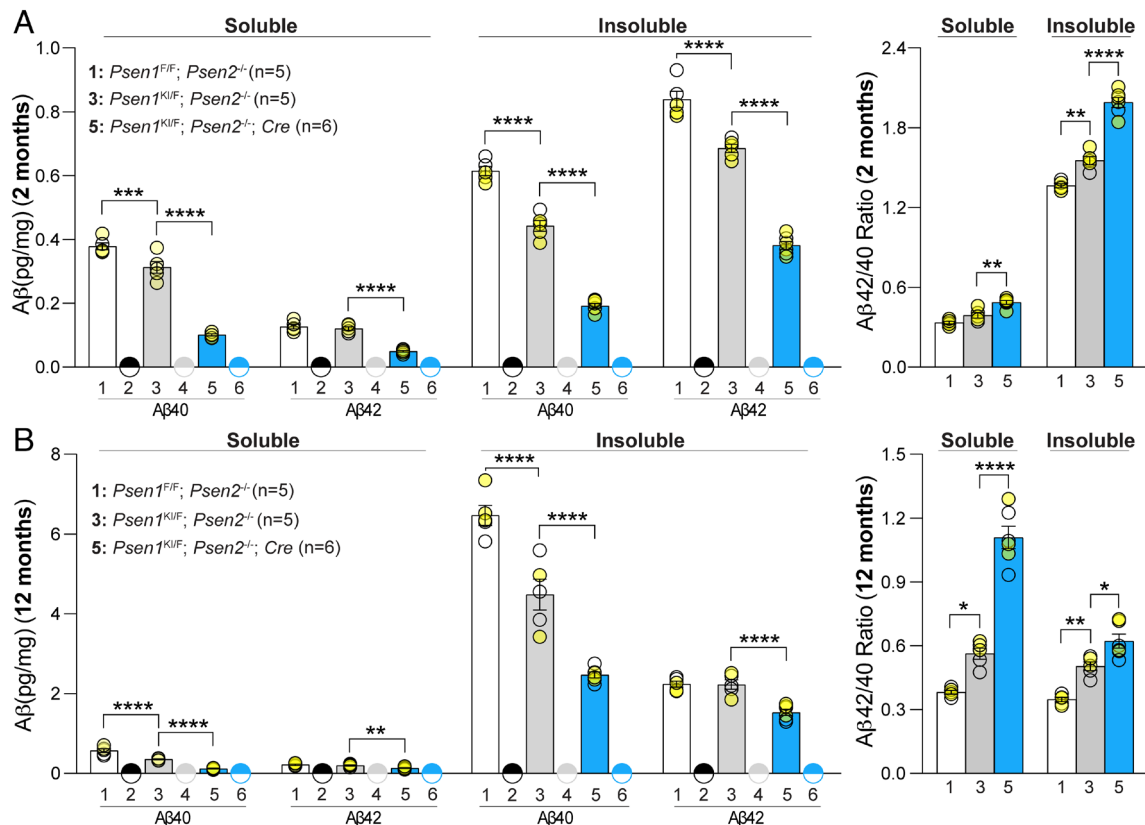


Fig. 2. Reduced A β levels and elevated A β 42/40 ratio in the cortex of L435F KI mice. (A) At 2 mo of age, in the soluble fraction, levels of A β 40 in the cerebral cortex of *Psen1*^{KI/F}; *Psen2*^{-/-}; *Cre* (0.10 \pm 0.00) are decreased, compared to *Psen1*^{KI/F}; *Psen2*^{-/-} (0.31 \pm 0.02; $F_{5,22} = 322.20$, $P < 0.0001$, one-way ANOVA with Tukey's post hoc comparisons) and *Psen1*^{F/F}; *Psen2*^{-/-} mice (0.38 \pm 0.01; $P < 0.0001$), and levels of A β 42 are also reduced in *Psen1*^{KI/F}; *Psen2*^{-/-}; *Cre* (0.05 \pm 0.00), relative to *Psen1*^{KI/F}; *Psen2*^{-/-} (0.12 \pm 0.01; $P < 0.0001$) and *Psen1*^{F/F}; *Psen2*^{-/-} (0.13 \pm 0.01; $P < 0.0001$). However, the A β 42/40 ratio is elevated in *Psen1*^{KI/F}; *Psen2*^{-/-}; *Cre* (0.49 \pm 0.01), compared to *Psen1*^{KI/F}; *Psen2*^{-/-} (0.39 \pm 0.02; $P = 0.0016$) and *Psen1*^{F/F}; *Psen2*^{-/-} (0.34 \pm 0.01; $P < 0.0001$). In the insoluble fraction, A β 40 shows a greater reduction in *Psen1*^{KI/F}; *Psen2*^{-/-}; *Cre* cortices (0.19 \pm 0.01), relative to *Psen1*^{KI/F}; *Psen2*^{-/-} (0.44 \pm 0.02; $P < 0.0001$) and *Psen1*^{F/F}; *Psen2*^{-/-} (0.61 \pm 0.02; $P < 0.0001$). More A β 42 were detected in the insoluble fraction, but levels of A β 42 are still significantly lower in *Psen1*^{KI/F}; *Psen2*^{-/-}; *Cre* cortices (0.38 \pm 0.01), compared to that in *Psen1*^{KI/F}; *Psen2*^{-/-} (0.69 \pm 0.01; $P < 0.0001$) and *Psen1*^{F/F}; *Psen2*^{-/-} (0.84 \pm 0.03; $P < 0.0001$). Similarly, the A β 42/40 ratio is elevated in *Psen1*^{KI/F}; *Psen2*^{-/-} cortices (1.55 \pm 0.03; $P = 0.003$) and is further enhanced in *Psen1*^{KI/F}; *Psen2*^{-/-}; *Cre* (1.99 \pm 0.04; $P < 0.0001$), compared to *Psen1*^{F/F}; *Psen2*^{-/-} mice (1.36 \pm 0.02). There is no detectable A β 40 and A β 42 in the soluble and insoluble fractions derived from cortices of *Psen1*^{F/F}; *Psen2*^{-/-}; *App*^{-/-} (Lane 2), *Psen1*^{KI/F}; *Psen2*^{-/-}; *App*^{-/-} (Lane 4), and *Psen1*^{KI/F}; *Psen2*^{-/-}; *Cre*; *App*^{-/-} (Lane 6). (B) At 12 mo of age, in the soluble fraction, levels of A β 40 are reduced in the cerebral cortex of *Psen1*^{KI/F}; *Psen2*^{-/-} mice (0.36 \pm 0.01; $P < 0.0001$) and are further decreased in *Psen1*^{KI/F}; *Psen2*^{-/-}; *Cre* (0.12 \pm 0.01), compared to *Psen1*^{F/F}; *Psen2*^{-/-} mice (0.57 \pm 0.04; $P < 0.0001$). Levels of A β 42 are decreased in *Psen1*^{KI/F}; *Psen2*^{-/-}; *Cre* (0.14 \pm 0.01), relative to *Psen1*^{KI/F}; *Psen2*^{-/-} (0.20 \pm 0.01; $P = 0.0031$) and *Psen1*^{F/F}; *Psen2*^{-/-} (0.22 \pm 0.02; $P = 0.0002$). However, the A β 42/40 ratio is elevated in *Psen1*^{KI/F}; *Psen2*^{-/-} (0.56 \pm 0.03; $P = 0.0156$) and is further increased in *Psen1*^{KI/F}; *Psen2*^{-/-}; *Cre* (1.11 \pm 0.05; $P < 0.0001$), compared to *Psen1*^{F/F}; *Psen2*^{-/-} (0.38 \pm 0.01). In the insoluble fraction, levels of A β 40 are reduced in *Psen1*^{KI/F}; *Psen2*^{-/-} (4.48 \pm 0.39; $P < 0.0001$) and further reduced in *Psen1*^{KI/F}; *Psen2*^{-/-}; *Cre* (2.47 \pm 0.07; $P < 0.0001$), relative to *Psen1*^{F/F}; *Psen2*^{-/-} (6.47 \pm 0.25). Levels of A β 42 are lower in *Psen1*^{KI/F}; *Psen2*^{-/-}; *Cre* (1.53 \pm 0.07; $P < 0.0001$) than in *Psen1*^{KI/F}; *Psen2*^{-/-} (2.23 \pm 0.12) and *Psen1*^{F/F}; *Psen2*^{-/-} mice (2.24 \pm 0.07). However, the A β 42/40 ratio is significantly enhanced in *Psen1*^{KI/F}; *Psen2*^{-/-} (0.50 \pm 0.02; $P = 0.0022$) and *Psen1*^{KI/F}; *Psen2*^{-/-}; *Cre* (0.62 \pm 0.03; $P = 0.0119$), compared to *Psen1*^{F/F}; *Psen2*^{-/-} cortices (0.35 \pm 0.01). There is no detectable A β 40 and A β 42 in the soluble and insoluble fractions derived from cortices of *Psen1*^{F/F}; *Psen2*^{-/-}; *App*^{-/-} (Lane 2), *Psen1*^{KI/F}; *Psen2*^{-/-}; *App*^{-/-} (Lane 4), and *Psen1*^{KI/F}; *Psen2*^{-/-}; *Cre*; *App*^{-/-} (Lane 6). All data represent means \pm SEM. * $P < 0.05$; ** $P < 0.01$; *** $P < 0.001$; **** $P < 0.0001$. $N = 5$ to 6 mice used in each experiment. Yellow-filled and open circles represent data obtained from individual male and female mice, respectively.

Levels of A β 42 are much higher in the insoluble fraction of all three genotypic groups, compared to the soluble fractions, and are significantly reduced in *Psen1*^{KI/F}; *Psen2*^{-/-} mice (0.69 \pm 0.01; $P < 0.0001$) and further decreased in *Psen1*^{KI/F}; *Psen2*^{-/-}; *Cre* mice (0.38 \pm 0.01; $P < 0.0001$), compared to controls (0.84 \pm 0.03; Fig. 2A). The greater reduction of A β 40, relative to A β 42, leads to increased A β 42/A β 40 ratio in *Psen1*^{KI/F}; *Psen2*^{-/-} (1.55 \pm 0.03, $P = 0.003$) and *Psen1*^{KI/F}; *Psen2*^{-/-}; *Cre* mice (1.99 \pm 0.03, $P < 0.0001$), compared to *Psen1*^{F/F}; *Psen2*^{-/-} (1.36 \pm 0.02; Fig. 2A). No A β 40 or A β 42 was detected in the cortex of *Psen1*^{F/F}; *Psen2*^{-/-}; *App*^{-/-}, *Psen1*^{KI/F}; *Psen2*^{-/-}; *App*^{-/-}, and *Psen1*^{KI/F}; *Psen2*^{-/-}; *Cre*; *App*^{-/-} mice (Fig. 2A).

An in vitro γ -secretase assay using CHAPSO solubilized membrane fractions from dissected cortices, which retain γ -secretase activity, and recombinant Notch substrates showed that the de novo production of NICD is significantly reduced in *Psen1*^{KI/F}; *Psen2*^{-/-} (-45%) and *Psen1*^{KI/F}; *Psen2*^{-/-}; *Cre* mice (-78%),

compared to littermate *Psen1*^{F/F}; *Psen2*^{-/-} controls ($P < 0.0001$; one-way ANOVA with Tukey's post hoc comparisons; *SI Appendix, Fig. S3A*). Using a recombinant APP substrate C99 followed by ELISA measurements of A β 40 and A β 42, we further found decreased de novo generation of A β 40 (-64%) and A β 42 (-35%) in *Psen1*^{KI/F}; *Psen2*^{-/-} cerebral cortices (A β 40: 258.00 \pm 9.62; $P < 0.0001$; A β 42: 139.20 \pm 3.83; $P = 0.0002$), compared to *Psen1*^{F/F}; *Psen2*^{-/-} (A β 40: 709.20 \pm 92.83; A β 42: 213.90 \pm 21.48), and further reduced in *Psen1*^{F/F}; *Psen2*^{-/-}; *Cre* brains (A β 40: -87%, 89.98 \pm 8.79; $P = 0.0004$; A β 42: -74%, 54.97 \pm 1.76; $P < 0.0001$; *SI Appendix, Fig. S3B*). The A β 42/A β 40 ratio is increased in *Psen1*^{KI/F}; *Psen2*^{-/-} mice (0.54 \pm 0.01; $P = 0.0026$) and *Psen1*^{KI/F}; *Psen2*^{-/-}; *Cre* mice (0.64 \pm 0.04; $P = 0.0001$), compared to the control (0.31 \pm 0.05). Western analysis confirmed that levels of PS1 CTF are significantly reduced in the cortex of *Psen1*^{KI/F}; *Psen2*^{-/-} mice ($P = 0.0292$) and further decreased in *Psen1*^{KI/F}; *Psen2*^{-/-}; *Cre* mice ($P < 0.0001$), whereas APP CTFs accumulate

in *Psen1^{K1/F}; Psen2^{-/-}; Cre* mice, consistent with decreased γ -secretase activity in these mice (SI Appendix, Fig. S3 C and D).

At 12 mo of age, A β levels accumulate greatly in the insoluble fraction, compared to those in the soluble fraction (Fig. 2B). A β 40 levels are reduced in the soluble (0.36 ± 0.01 ; $P < 0.0001$) and insoluble (4.48 ± 0.39 ; $P < 0.0001$) fractions derived from the cortex of *Psen1^{K1/F}; Psen2^{-/-}* mice, relative to *Psen1^{F/F}; Psen2^{-/-}* mice (soluble: 0.57 ± 0.04 ; insoluble: 6.47 ± 0.25), and further reduced in *Psen1^{K1/F}; Psen2^{-/-}; Cre* mice ($P < 0.0001$), whereas A β 42 levels are reduced in *Psen1^{K1/F}; Psen2^{-/-}; Cre* mice ($P < 0.0001$), relative to *Psen1^{F/F}; Psen2^{-/-}* mice (Fig. 2B). The greater reduction in A β 40, relative to A β 42, results in increases of A β 42/A β 40 in the soluble and insoluble fractions from *Psen1^{K1/F}; Psen2^{-/-}* and *Psen1^{K1/F}; Psen2^{-/-}; Cre* cortices, compared to *Psen1^{F/F}; Psen2^{-/-}* controls (Fig. 2B).

APP Deficiency Does Not Rescue Increased Apoptosis in the Cortex of *Psen* Mutant Mice. We also examined the effects of APP deficiency on increases of apoptosis in *Psen* mutant mice by performing immunostaining using antibodies against active Caspase-3 to label apoptotic cells in brain sections of all eight genotypic groups at the ages of 2, 12, and 18 mo (Fig. 3A and SI Appendix, Fig. S4A). Stereological quantification of active Caspase-3+ apoptotic cells in the neocortex of these eight genotypic groups showed genotype-specific increases at all three age groups ($F_{14,66} = 8.05$, $P < 0.0001$; two-way ANOVA). At 2 mo of age, the number of active Caspase-3+ apoptotic cells is significantly higher in the neocortex of *Psen1^{K1/F}; Psen2^{-/-}; Cre* mice (647 ± 28 ; $P < 0.0001$, two-way ANOVA with Tukey's post hoc comparisons), relative to *Psen1^{K1/F}; Psen2^{-/-}* (287 ± 26) and *Psen1^{F/F}; Psen2^{-/-}* mice (257 ± 31), but the number is similar to that in *Psen1^{K1/F}; Psen2^{-/-}; Cre; App^{-/-}* mice (632 ± 34 ; $P > 0.99$),

indicating that the lack of APP or A β does not rescue the increase in apoptotic cell death in the cerebral cortex of *Psen1^{K1/F}; Psen2^{-/-}; Cre* mice (Fig. 3B and SI Appendix, Fig. S4B). The number of apoptotic cells is further increased in the neocortex of *Psen* cDKO mice ($1,047 \pm 48$), compared to *Psen1^{K1/F}; Psen2^{-/-}; Cre* mice (647 ± 28 ; $P < 0.0001$), but the number is not different from that in *Psen* cDKO; *App^{-/-}* mice ($1,060 \pm 71$; $P > 0.99$). Similarly, quantification of TUNEL+ cells also showed increases of apoptotic cells in the cortex of *Psen1^{K1/F}; Psen2^{-/-}; Cre* mice ($1,393 \pm 70$) and *Psen* cDKO mice ($2,375 \pm 110$) at 2 mo of age, compared to control groups ($P < 0.0001$), but APP deficiency has no impact on the number of apoptotic cells ($P > 0.99$; SI Appendix, Fig. S5). Even though the increase in TUNEL+ apoptotic cells is already dramatic in the neocortex of *Psen1^{K1/F}; Psen2^{-/-}; Cre* mice (three-fold) and *Psen* cDKO mice (five-fold) at 2 mo of age, compared to control mice, apoptotic cells represent a very small percentage (<0.1%) of NeuN+ cortical neurons (SI Appendix, Fig. S5B). Thus, the number of cortical neurons is not significantly reduced in *Psen1^{K1/F}; Psen2^{-/-}; Cre* and *Psen* cDKO mice at this age (SI Appendix, Fig. S1).

At 12 mo of age, the number of apoptotic cells in the neocortex of *Psen1^{K1/F}; Psen2^{-/-}; Cre* mice (960 ± 52) is more dramatically increased than those at 2 mo of age (647 ± 28 ; $P = 0.0015$) but the number of apoptotic cells is similar in the neocortex between *Psen1^{K1/F}; Psen2^{-/-}; Cre* and *Psen1^{K1/F}; Psen2^{-/-}; Cre; App^{-/-}* mice (993 ± 62 ; $P > 0.99$), indicating that lack of APP has no impact on the increased apoptosis (Fig. 3B). The increase of apoptotic cells is most dramatic in the neocortex of *Psen* cDKO mice at the age of 12 mo ($1,380 \pm 59$), but the number of apoptotic cells is still similar between *Psen* cDKO and *Psen* cDKO; *App^{-/-}* mice ($1,427 \pm 74$; $P > 0.99$; SI Appendix, Fig. S4B). By 18 mo of age, enhanced apoptosis in the neocortex of *Psen1^{K1/F}; Psen2^{-/-}; Cre*

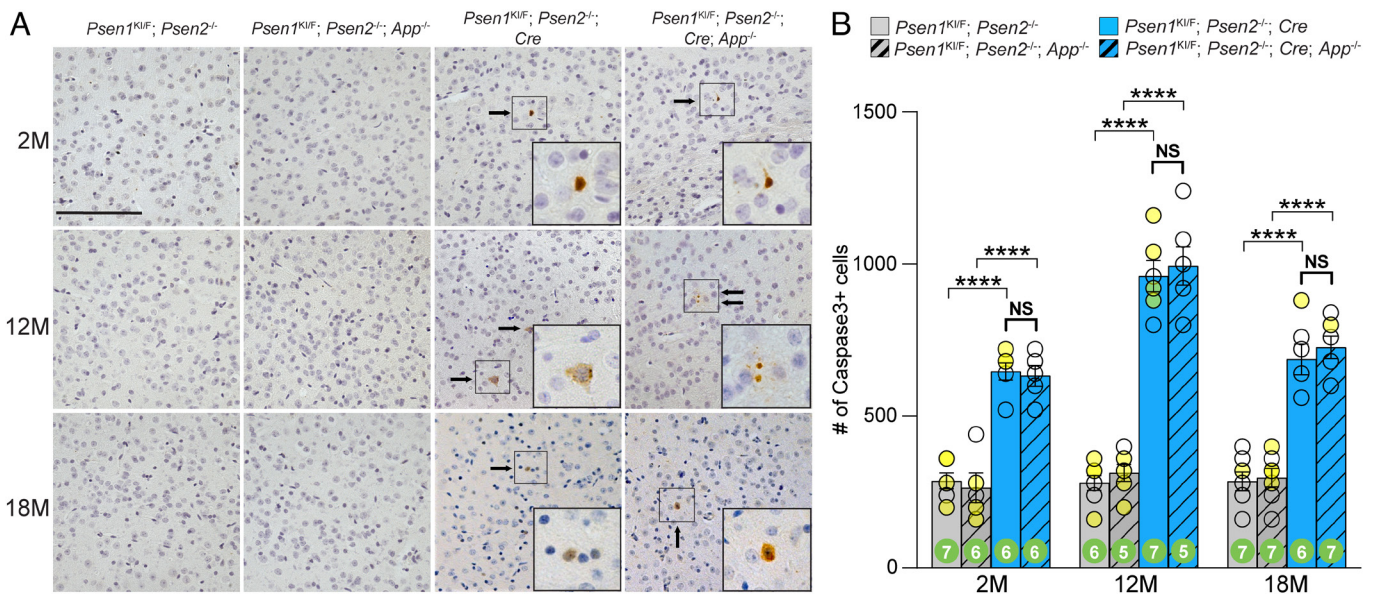


Fig. 3. APP deficiency does not rescue increases of apoptosis in the cortex of L435F KI mice. (A) Active Caspase-3 immunostaining of comparable sagittal sections of four indicated genotypic groups at the ages of 2, 12, and 18 mo shows increases of apoptotic cells in the cerebral cortex of *Psen1^{K1/F}; Psen2^{-/-}; Cre* and *Psen1^{K1/F}; Psen2^{-/-}; Cre; App^{-/-}* mice at all ages examined. The inserts show higher-power views of the boxed areas. (Scale bar, 100 μ m.) (B) Stereological quantification shows genotype-specific, age-dependent increases of apoptotic cells in the neocortex ($F_{14,66} = 8.05$, $P < 0.0001$, two-way ANOVA). At 2 mo of age, the number of active Caspase-3+ cells in the neocortex of *Psen1^{K1/F}; Psen2^{-/-}; Cre* (647 ± 28) is significantly increased (2.2-fold), relative to *Psen1^{K1/F}; Psen2^{-/-}* mice (287 ± 26 ; $P < 0.0001$, two-way ANOVA with Tukey's post hoc comparisons). However, the number of active Caspase-3+ cells is similar between *Psen1^{K1/F}; Psen2^{-/-}; Cre* (647 ± 28) and *Psen1^{K1/F}; Psen2^{-/-}; Cre; App^{-/-}* mice (632 ± 34 ; $P > 0.99$). At 12 mo of age, the number of apoptotic cells in *Psen1^{K1/F}; Psen2^{-/-}; Cre* mice (960 ± 52) is markedly increased (3.4-fold), relative to *Psen1^{K1/F}; Psen2^{-/-}* mice (280 ± 25 ; $P < 0.0001$). The increase of apoptosis in *Psen1^{K1/F}; Psen2^{-/-}; Cre* mice at 12 mo (3.4-fold) is more dramatic than those at 2 mo of age (2.2-fold). However, the number of active Caspase-3+ cells is similar between *Psen1^{K1/F}; Psen2^{-/-}; Cre* mice (960 ± 52) and *Psen1^{K1/F}; Psen2^{-/-}; Cre; App^{-/-}* mice (993 ± 62 ; $P > 0.99$). At 18 mo of age, more active Caspase-3+ cells are present in the neocortex of *Psen1^{K1/F}; Psen2^{-/-}; Cre* mice (687 ± 51), relative to *Psen1^{K1/F}; Psen2^{-/-}* mice (286 ± 30 ; $P < 0.0001$). Again, the number of active Caspase-3+ cells is similar between *Psen1^{K1/F}; Psen2^{-/-}; Cre* (687 ± 51) and *Psen1^{K1/F}; Psen2^{-/-}; Cre; App^{-/-}* mice (726 ± 34 ; $P > 0.99$). All data represent means \pm SEM. **** $P < 0.0001$; NS, not significant. The value in the column indicates the number of mice used in each experiment. Yellow-filled and open circles represent data obtained from individual male and female mice, respectively.

(687 ± 51) and *Psen* cDKO (847 ± 80) mice is less dramatic than those at 12 mo of age (Fig. 3B and *SI Appendix, Fig. S4B*). Still the number of apoptotic cells is similar between *Psen1^{K1/F}; Psen2^{-/-}; Cre* (687 ± 51) and *Psen1^{K1/F}; Psen2^{-/-}; Cre; App^{-/-}* mice (726 ± 34; $P > 0.99$), and between *Psen* cDKO (847 ± 80) and *Psen* cDKO; *App^{-/-}* mice (887 ± 43; $P > 0.99$; *SI Appendix, Fig. S4B*), further supporting that APP deficiency does not affect increased apoptosis observed in *Psen* mutant mice.

APP Deficiency Has No Impact on Microgliosis in *Psen* Mutant Mice.

We further evaluated the effects of APP deficiency on the progressive microgliosis in the cerebral cortex of *Psen* mutant mice by performing immunostaining using antibodies against Iba1 to label microglia in brain sections of all eight genotypes at the ages of 2, 12, and 18 mo (Fig. 4A and *SI Appendix, Fig. S6A*). Stereological quantification of Iba1+ cells in the neocortex of these eight genotypic groups showed age-dependent, genotypic-specific differences ($F_{14,67} = 161.30$, $P < 0.0001$; two-way ANOVA with Tukey's post hoc comparisons). At 2 mo of age, the density of Iba1+ cells in the neocortex of *Psen1^{K1/F}; Psen2^{-/-}; Cre* mice ($13.02 \pm 0.26 \times 10^3$ cells/mm³) is similar to that in *Psen1^{K1/F}; Psen2^{-/-}* ($12.05 \pm 0.30 \times 10^3$ cells/mm³; $P > 0.99$), but the density of microglia in *Psen* cDKO mice ($15.69 \pm 0.49 \times 10^3$ cells/mm³) is significantly higher than that in *Psen1^{F/F}; Psen2^{-/-}* mice ($11.68 \pm 0.36 \times 10^3$ cells/mm³; $P = 0.0018$), suggesting elevated microgliosis at this age in *Psen* cDKO mice (*SI Appendix, Fig. S6B*).

At 12 mo of age, the density of Iba1+ microglia in the neocortex of *Psen1^{K1/F}; Psen2^{-/-}; Cre* mice ($24.82 \pm 0.55 \times 10^3$ cells/mm³) is significantly increased, relative to *Psen1^{K1/F}; Psen2^{-/-}* ($12.12 \pm 0.39 \times 10^3$ cells/mm³; $P < 0.0001$) and *Psen1^{F/F}; Psen2^{-/-}* ($12.10 \pm 0.53 \times 10^3$ cells/mm³; $P < 0.0001$), but the microglial density is not significantly different between *Psen1^{K1/F}; Psen2^{-/-}; Cre* ($24.82 \pm 0.55 \times 10^3$ cells/mm³) and *Psen1^{K1/F}; Psen2^{-/-}; Cre; App^{-/-}* mice ($25.26 \pm 0.49 \times 10^3$

cells/mm³; $P > 0.99$; Fig. 4B and *SI Appendix, Fig. S6B*). Moreover, microgliosis is further exacerbated in *Psen* cDKO mice ($37.52 \pm 0.65 \times 10^3$ cells/mm³), but there is no difference between *Psen* cDKO and *Psen* cDKO; *App^{-/-}* mice ($39.02 \pm 0.53 \times 10^3$ cells/mm³; $P > 0.99$; *SI Appendix, Fig. S6B*). At 18 mo of age, the density of microglia is further enhanced in the neocortex of *Psen1^{K1/F}; Psen2^{-/-}; Cre* mice ($30.18 \pm 0.72 \times 10^3$ cells/mm³), relative to *Psen1^{K1/F}; Psen2^{-/-}* mice ($12.79 \pm 0.58 \times 10^3$ cells/mm³; $P < 0.0001$) and *Psen1^{F/F}; Psen2^{-/-}* ($12.41 \pm 0.50 \times 10^3$ cells/mm³; $P < 0.0001$), but there is no difference between *Psen1^{K1/F}; Psen2^{-/-}; Cre* ($30.18 \pm 0.72 \times 10^3$ cells/mm³) and *Psen1^{K1/F}; Psen2^{-/-}; Cre; App^{-/-}* mice ($29.51 \pm 0.80 \times 10^3$ cells/mm³; $P > 0.99$) or between *Psen* cDKO ($48.80 \pm 0.88 \times 10^3$ cells/mm³) and *Psen* cDKO; *App^{-/-}* mice ($50.12 \pm 0.16 \times 10^3$ cells/mm³; $P > 0.99$; *SI Appendix, Fig. S6B*), indicating that removal of APP or A β does not affect microgliosis in *Psen* mutant mice.

Discussion

More than 450 mutations, mostly missense mutations scattering throughout the coding sequences of *PSEN1* and *PSEN2*, have been reported (alzforum.org/mutations), highlighting the importance of PS in AD pathogenesis. The initial discovery of increased A β 42/A β 40 in transgenic mice and FAD patients carrying *PSEN1* mutations suggested that these mutations might cause FAD *via* a toxic gain-of-function pathogenic mechanism (7, 8), providing key additional evidence for the amyloid hypothesis (9). However, the broad distribution of the large number of distinct mutations is also consistent with a loss-of-function pathogenic mechanism. Genetic findings from conditional knockout studies revealed an essential role of PS in learning and memory, synaptic plasticity, and age-dependent neuronal survival (10–12, 16), leading to the proposal of the presenilin hypothesis, which posits that *PSEN* mutations may cause loss of its essential function, resulting in

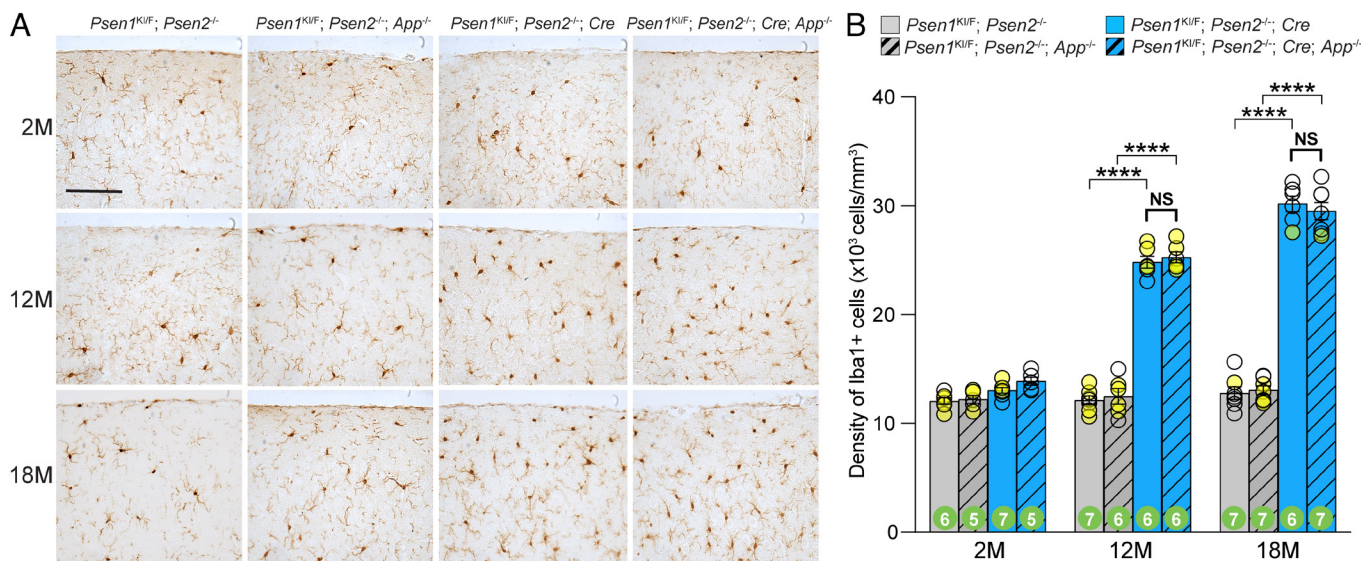


Fig. 4. APP deficiency has no effect on elevated microgliosis caused by the *Psen1* L435F KI allele. (A) Iba1 immunostaining of comparable brain sections of *Psen1^{K1/F}; Psen2^{-/-}; Cre* and *Psen1^{K1/F}; Psen2^{-/-}; Cre; App^{-/-}* mice and controls at the ages of 2, 12, and 18 mo shows age-dependent increases of microgliosis in the cerebral cortex of *Psen1^{K1/F}; Psen2^{-/-}; Cre* and *Psen1^{K1/F}; Psen2^{-/-}; Cre; App^{-/-}* mice. (Scale bar, 100 μ m.) (B) Stereological quantification of Iba1+ cells in the four genotypic groups at the ages of 2, 12, and 18 mo shows significant age-dependent, genotype-dependent increases of microglia ($F_{14,67} = 161.30$, $P < 0.0001$; two-way ANOVA with Tukey's post hoc comparisons). At 2 mo of age, the density of Iba1+ cells is similar among four genotypic groups ($P > 0.99$). At 12 mo of age, the density of Iba1+ microglia is significantly higher in the neocortex of *Psen1^{K1/F}; Psen2^{-/-}; Cre* ($24.82 \pm 0.55 \times 10^3$ cells/mm³), relative to *Psen1^{K1/F}; Psen2^{-/-}* mice ($12.12 \pm 0.39 \times 10^3$ cells/mm³; $P < 0.0001$), but the density of Iba1+ microglia is similar between *Psen1^{K1/F}; Psen2^{-/-}; Cre* and *Psen1^{K1/F}; Psen2^{-/-}; Cre; App^{-/-}* mice ($25.26 \pm 0.49 \times 10^3$ cells/mm³; $P > 0.99$). At 18 mo of age, the density of Iba1+ microglia is further increased in the neocortex of *Psen1^{K1/F}; Psen2^{-/-}; Cre* mice ($30.18 \pm 0.72 \times 10^3$ cells/mm³), relative to *Psen1^{K1/F}; Psen2^{-/-}* mice ($12.79 \pm 0.58 \times 10^3$ cells/mm³; $P < 0.0001$), but the density of Iba1+ microglia is similar between *Psen1^{K1/F}; Psen2^{-/-}; Cre* and *Psen1^{K1/F}; Psen2^{-/-}; Cre; App^{-/-}* ($29.51 \pm 0.80 \times 10^3$ cells/mm³; $P > 0.99$). All data represent means \pm SEM. **** $P < 0.0001$; NS, not significant. The value in the column indicates the number of mice used in each experiment. Yellow-filled and open circles represent data obtained from individual male and female mice, respectively.

neurodegeneration and dementia in FAD (23). The presenilin hypothesis was substantiated by subsequent studies that demonstrated that *PSEN* mutations result in loss of γ -secretase activity in cultured cells, KI mice, and in vitro biochemical systems (24–30) and that reduced PS expression in conditional mutant mice and *Psn* knockdown flies also causes increases of apoptosis and age-dependent neurodegeneration in a PS dose-dependent manner (13–15, 33–35).

The increase of A β 42/A β 40 by *PSEN* mutations in transgenic and KI mice as well as FAD patients, however, raised the possibility that elevated A β 42/A β 40 may trigger or contribute to neurodegeneration in *Psen* mutant mice, even though A β production is decreased (24–30). Given the importance of the debate and the consequential opposing therapeutic intervention, our current study aims to address this question conclusively. We employ a genetic approach to remove A β completely and then compare the consequences of *Psen1* L435F KI and conditional null alleles in the presence or the absence of APP. Complementary neuropathological analysis of eight genotypic groups at three different ages (2, 12, 18 mo) showed that removal of A β by APP deficiency has no impact on the age-dependent reduction of cortical volume as well as progressive losses of cortical neurons caused by *Psen1* L435F KI and null alleles, despite the increase in the ratio of A β 42/A β 40 in the presence of APP (Figs. 1 and 2 and *SI Appendix, Figs. S1 and S3*). Furthermore, APP deficiency does not rescue elevated apoptotic cell death in the cerebral cortex of various *Psen* mutant mice at the ages of 2, 12, and 18 mo, nor does it alleviate microgliosis in *Psen* mutant mice (Figs. 3 and 4 and *SI Appendix, Figs. S4–S6*). These findings demonstrate that *Psen* mutations cause neurodegeneration independent of A β , providing further experimental evidence in support of the presenilin hypothesis.

The isolation of A β peptides and the identification of its protein sequences in 1984 sparked interest in the role of A β in AD pathogenesis (36, 37). The subsequent linkage of APP mutations to FAD provided further genetic evidence (6), and the discovery that *PSEN* mutations increased the ratio of A β 42/A β 40 in FAD patients and transgenic mice (7, 8) cemented the predominance of the amyloid hypothesis and the corresponding intense focus on anti-amyloid therapies (9). However, the amyloid hypothesis is inconsistent with several lines of experimental evidence (23). For example, the distribution and load of amyloid plaques correlate poorly with the severity of dementia, whereas synaptic loss correlates well with the clinical features of dementia (38). Moreover, APP transgenic mice overexpressing various human mutant APP do not develop prominent neurodegeneration, despite accumulation of very high levels of A β including A β 42 and amyloid plaques in the cerebral cortex (39). Interestingly, in contrast to striking age-dependent neurodegeneration in the cerebral cortex of *Psen* mutant mice (Figs. 1, 3, and 4 and *SI Appendix, Figs. S1 and S4–S6*), excitatory neuron-specific *App/Aplp1/Aplp2* conditional triple knockout mice using the same Cre line develop no neurodegeneration even at ~2 y of age (40), suggesting that APP mutations cause AD via a distinct mechanism from *PSEN* mutations.

Genetic studies using cell type-specific conditional knockout mice demonstrated an essential role of PS in learning and memory, synaptic plasticity, and age-dependent neuronal survival (10–13, 15–22). Moreover, partial loss of PS function in excitatory neurons of the postnatal forebrain also results in age-dependent cortical neuronal loss and increases of apoptosis though to a lesser extent and at a later age of onset (33), relative to complete inactivation of PS (10). Furthermore, the essential role of PS in support of neuronal survival in the aging brain is conserved from *Drosophila* to mammals, as conditional knockdown of the *Drosophila* homologue, *Psn*, also results in age-dependent neurodegeneration,

increases of apoptosis, behavioral deficits, and earlier mortality (34, 35). Together, these studies using loss-of-function mutants demonstrated an evolutionarily conserved, essential function of PS in processes highly relevant to AD, providing an initial premise for the presenilin hypothesis.

Using a sensitive, quantitative cell culture system, we initially found that all *Psen1* mutations tested result in partial to near complete loss of γ -secretase activity with the L435F mutation causing the most dramatic loss of γ -secretase activity, and that mutant PS1 exerts a dominant negative effect and inhibits γ -secretase activity of wild-type PS1 in trans (24, 25). Subsequent genetic analysis demonstrated striking resemblances of *Psen1* L435F and C410Y homozygous KI mice to *Psen1*-null mice, including perinatal lethality, neurogenesis impairment, reduced Notch signaling, and undetectable γ -secretase activity and A β production (26, 27). Furthermore, the L435F KI allele results in synaptic and memory impairments and age-dependent neurodegeneration, similar to but less severe than those caused by complete inactivation of PS in *Psen* cDKO mice, suggesting that the L435F KI allele retains residual PS function despite undetectable levels of γ -secretase activity (10, 26, 28). Indeed, high-resolution structural analysis of the γ -secretase complex placed the side chain of the L435 residue between D257 and D385, the two aspartate residues that constitute the active site of γ -secretase (41), providing an independent structural explanation for the severe loss of function phenotypes exhibited by L435F. Finally, a large-scale biochemical study of 138 *PSEN1* mutations showed that ~90% of mutations cause loss of γ -secretase activity with ~30% of mutations abolishing its activity (29, 30). Thus, these studies in cell culture, KI mice, and in vitro biochemical systems all demonstrated that *PSEN* mutations impair γ -secretase activity, providing additional experimental evidence for the presenilin hypothesis.

The current study further shows unequivocally that the neurodegeneration phenotypes caused by *Psen* mutations are independent of A β . While the *Psen1* L435F mutation exhibits no detectable γ -secretase activity in homozygous KI brains, residual levels (~10%) of PS1 NTF and CTF are detected, suggesting that despite its proximity to the active site of γ -secretase, L435F retains residual PS function (10, 26, 28–30). Consistent with this notion, the L435F KI allele causes less severe hippocampal synaptic and memory deficits as well as age-dependent neurodegeneration in the cerebral cortex (10, 26, 28), compared to the *Psen1* conditional null allele (Fig. 1 and *SI Appendix, Fig. S1*).

Despite the cell intrinsic, essential role of PS in the survival of excitatory and inhibitory neurons in the cerebral cortex (10, 11, 13, 15, 28), the molecular mechanism by which PS supports neuronal survival is less clear. With only <0.1% of cortical neurons undergoing apoptosis at any given time (Fig. 3 and *SI Appendix, Fig. S5*), it is challenging to identify relevant molecular changes in the cortex of *Psen* mutant mice. Employing a genetic approach in *Drosophila* by developing inducible neuron-specific *Psn* knockdown flies, we identified several genes encoding lipid transporters and receptors that interact with Psn-dependent neuronal survival, highlighting the importance of lipid metabolism in aging and neurodegeneration (35). While single-cell RNA sequencing of cortical samples dissected from these unique excitatory or inhibitory neuron-specific *Psen* mutant mice at multiple ages may reveal cell intrinsic transcriptomic changes, the relevance of the identified molecular changes would require genetic validation to confirm their roles in support of PS-dependent neuronal survival during aging, which could be further explored for therapeutic development.

Targeting A β has been the predominant therapeutic effort by major pharmaceutical companies over the last 25 y (42), cumulating to the full approval of lecanemab, an anti-A β antibody, by the FDA

for AD treatment. However, despite the dramatic improvement of amyloid burden by lecanemab, patients continued their clinical decline, albeit in a slightly less steep progression, raising additional questions (43). The poor clinical efficacy and the significant risk of developing cerebral bleeding may explain the very limited use of lecanemab since its approval. Ultimately, clinical effectiveness of any new therapies would determine their utility based on their ability to improve AD patients' quality of life.

Materials and Methods

Mice. All animal procedures were approved by the Institutional Animal Care and Use Committee (IACUC) at the Brigham and Women's Hospital in accordance with the USDA Animal Welfare Act and PHS Policy on Humane Care and Use of Laboratory Animals. Mice were maintained on a 12-h light/dark cycle and were provided with standard rodent chow and water. Mice of both sexes at the ages of 2, 12, and 18 mo were used for phenotypic analysis. Generation and multidisciplinary characterization of *Psen1* L435F KI, floxed *Psen1*, *App*^{-/-}, and *Psen* cDKO mice were previously described (9, 15, 25, 38). The eight genotypic groups used in the current study were obtained from breeding pairs of *Psen1*^{Fl/F}; *Psen2*^{-/-}; *App*^{+/-} and *Psen1*^{Kl/F}; *Psen2*^{-/-}; *App*^{+/-}; *Cre* or *Psen1*^{Fl/F}; *Psen2*^{-/-}; *App*^{+/-}; *Cre* and *Psen1*^{Kl/F}; *Psen2*^{-/-}; *App*^{+/-} mice. The *Camk2a-Cre* (*Cre*) transgene is expressed selectively in excitatory neurons of the postnatal forebrain and drives *Cre*-mediated deletions of the floxed *Psen1* alleles into null alleles in excitatory neurons of the cerebral cortex beginning at postnatal day 18 (9, 15, 16). All mutant mice were maintained in the C57BL6/129 hybrid background by breeding to wild-type C57BL6/129 F1 mice periodically (three to four generations), and all eight experimental genotypic groups were obtained from the same breeding pairs.

Neuropathological Analysis, ELISA, and Western Blotting. Quantitative immunohistochemical analysis was performed using one brain hemisphere as described previously (15, 26, 40, 44), and the detailed information can be found in *SI Appendix, Materials and Methods*. Dissected cortices from the other hemisphere were analyzed using the ELISA or western blotting as described before

(15, 26, 28, 40), and detailed methods can be found in *SI Appendix, Materials and Methods*. All antibodies used in the current study are described in *SI Appendix, Materials and Methods* and Table S1.

Data Quantification and Statistical Analysis. Data acquisition and quantification were performed in a genotype-blind manner with the exception of molecular analysis (Western, ELISA). All statistical analysis was performed using Prism (Version 10; GraphPad), Excel (Microsoft), or Clampfit (Version 10.3; Molecular device). All data are presented as the mean ± SEM. The exact sample size (e.g., the number of mice) of each experiment is indicated in the figure. Statistical analysis was conducted using two-way ANOVA followed by Tukey's post hoc multiple comparisons (Figs. 1, 3, and 4 and *SI Appendix, Figs. S1, S4, and S6*), two-way ANOVA followed by Bonferroni's post hoc comparisons (*SI Appendix, Fig. S2*), one-way ANOVA followed by Tukey's post hoc multiple comparisons (Fig. 2 and *SI Appendix, Figs. S3 and S5*). All statistical comparisons were performed on the data from biologically independent samples. Significance is shown as **P* < 0.05, ***P* < 0.01, ****P* < 0.001, *****P* < 0.0001, or NS, not significant.

Data, Materials, and Software Availability. All data are included in the manuscript and/or *SI Appendix*.

ACKNOWLEDGMENTS. We would like to thank Huailong Zhao for technical assistance and other Shen lab members for discussion and coding the brain samples. This work was supported by grants from the NIH (R01NS041783 and RF1AG063520 to J.S.).

Author affiliations: ^aDepartment of Neurology, Brigham and Women's Hospital, Harvard Medical School, Boston, MA 02115; and ^bProgram in Neuroscience, Harvard Medical School, Boston, MA 02115

Author contributions: K.Y. and J.S. designed research; K.Y., J.K., and P.M. performed research; K.Y., C.Z., J.K., and P.M. analyzed data; K.Y. performed the neuropathological analysis; C.Z. verified all raw data, performed validation experiments, and prepared figures; J.K. performed ELISA; P.M. performed Western blotting; J.S. conceived and directed the project; and K.Y., C.Z., and J.S. wrote the paper.

1. R. Sherrington *et al.*, Cloning of a gene bearing missense mutations in early-onset familial Alzheimer's disease. *Nature* **375**, 754–760 (1995).
2. E. I. Rogaeve *et al.*, Familial Alzheimer's disease in kindreds with missense mutations in a gene on chromosome 1 related to the Alzheimer's disease type 3 gene. *Nature* **376**, 775–778 (1995).
3. B. De Strooper *et al.*, Deficiency of presenilin-1 inhibits the normal cleavage of amyloid precursor protein. *Nature* **391**, 387–390 (1998).
4. B. De Strooper *et al.*, A presenilin-1-dependent gamma-secretase-like protease mediates release of Notch intracellular domain. *Nature* **398**, 518–522 (1999).
5. W. Song *et al.*, Proteolytic release and nuclear translocation of Notch-1 are induced by presenilin-1 and impaired by pathogenic presenilin-1 mutations. *Proc. Natl. Acad. Sci. U.S.A.* **96**, 6959–6963 (1999).
6. A. Goate *et al.*, Segregation of a missense mutation in the amyloid precursor protein gene with familial Alzheimer's disease. *Nature* **349**, 704–706 (1991).
7. K. Duff *et al.*, Increased amyloid-beta42(43) in brains of mice expressing mutant presenilin 1. *Nature* **383**, 710–713 (1996).
8. D. Scheuner *et al.*, Secreted amyloid beta-protein similar to that in the senile plaques of Alzheimer's disease is increased in vivo by the presenilin 1 and 2 and APP mutations linked to familial Alzheimer's disease. *Nat. Med.* **2**, 864–870 (1996).
9. J. Hardy, D. J. Selkoe, The amyloid hypothesis of Alzheimer's disease: Progress and problems on the road to therapeutics. *Science* **297**, 353–356 (2002).
10. C. A. Saura *et al.*, Loss of presenilin function causes impairments of memory and synaptic plasticity followed by age-dependent neurodegeneration. *Neuron* **42**, 23–36 (2004).
11. R. Feng *et al.*, Forebrain degeneration and ventricle enlargement caused by double knockout of Alzheimer's presenilin-1 and presenilin-2. *Proc. Natl. Acad. Sci. U.S.A.* **101**, 8162–8167 (2004).
12. V. Beglopoulos *et al.*, Reduced beta-amyloid production and increased inflammatory responses in presenilin conditional knock-out mice. *J. Biol. Chem.* **279**, 46907–46914 (2004).
13. M. Wines-Samuels *et al.*, Characterization of age-dependent and progressive cortical neuronal degeneration in presenilin conditional mutant mice. *PLoS ONE* **5**, e10195 (2010).
14. H. Watanabe, D. Xia, T. Kanekiyo, R. J. Kelleher III, J. Shen, Familial frontotemporal dementia-associated presenilin-1 c.548G>T mutation causes decreased mRNA expression and reduced presenilin function in knock-in mice. *J. Neurosci.* **32**, 5085–5096 (2012).
15. J. Kang, J. Shen, Cell-autonomous role of Presenilin in age-dependent survival of cortical interneurons. *Mol. Neurodegener.* **15**, 72 (2020).
16. H. Yu *et al.*, APP processing and synaptic plasticity in presenilin-1 conditional knockout mice. *Neuron* **31**, 713–726 (2001).
17. C. Zhang *et al.*, Presenilins are essential for regulating neurotransmitter release. *Nature* **460**, 632–636 (2009).
18. D. Zhang *et al.*, Inactivation of presenilins causes pre-synaptic impairment prior to post-synaptic dysfunction. *J. Neurochem.* **115**, 1215–1221 (2010).
19. B. Wu, H. Yamaguchi, F. A. Lai, J. Shen, Presenilins regulate calcium homeostasis and presynaptic function via ryanodine receptors in hippocampal neurons. *Proc. Natl. Acad. Sci. U.S.A.* **110**, 15091–15096 (2013).
20. S. H. Lee *et al.*, Presenilins regulate synaptic plasticity and mitochondrial calcium homeostasis in the hippocampal mossy fiber pathway. *Mol. Neurodegener.* **12**, 48 (2017).
21. S. H. Lee, V. Y. Bolshakov, J. Shen, Inactivation of Presenilin in inhibitory neurons results in decreased GABAergic responses and enhanced synaptic plasticity. *Mol. Brain* **14**, 85 (2021).
22. S. H. Lee, V. Y. Bolshakov, J. Shen, Presenilins regulate synaptic plasticity in the perforant pathways of the hippocampus. *Mol. Brain* **16**, 17 (2023).
23. J. Shen, R. J. Kelleher III, The presenilin hypothesis of Alzheimer's disease: Evidence for a loss-of-function pathogenic mechanism. *Proc. Natl. Acad. Sci. U.S.A.* **104**, 403–409 (2007).
24. E. A. Heilig, W. Xia, J. Shen, R. J. Kelleher III, A presenilin-1 mutation identified in familial Alzheimer disease with cotton wool plaques causes a nearly complete loss of gamma-secretase activity. *J. Biol. Chem.* **285**, 22350–22359 (2010).
25. E. A. Heilig, U. Gutti, T. Tai, J. Shen, R. J. Kelleher III, Trans-dominant negative effects of pathogenic PSEN1 mutations on gamma-secretase activity and Aβ production. *J. Neurosci.* **33**, 11606–11617 (2013).
26. D. Xia *et al.*, Presenilin-1 knockin mice reveal loss-of-function mechanism for familial Alzheimer's disease. *Neuron* **85**, 967–981 (2015).
27. D. Xia, R. J. Kelleher III, J. Shen, Loss of Aβ43 production caused by Presenilin-1 mutations in the knockin mouse brain. *Neuron* **90**, 417–422 (2016).
28. P. Montenegro *et al.*, Human Presenilin-1 delivered by AAV9 rescues impaired gamma-secretase activity, memory deficits, and neurodegeneration in Psen mutant mice. *Proc. Natl. Acad. Sci. U.S.A.* **120**, e2306714120 (2023).
29. L. Sun, R. Zhou, G. Yang, Y. Shi, Analysis of 138 pathogenic mutations in presenilin-1 on the in vitro production of Aβ42 and Aβ40 peptides by gamma-secretase. *Proc. Natl. Acad. Sci. U.S.A.* **114**, E476–E485 (2017).
30. R. Zhou, G. Yang, Y. Shi, Dominant negative effect of the loss-of-function gamma-secretase mutations on the wild-type enzyme through heterooligomerization. *Proc. Natl. Acad. Sci. U.S.A.* **114**, 12731–12736 (2017).
31. G. Woodruff *et al.*, The presenilin-1 ΔE9 mutation results in reduced gamma-secretase activity, but not total loss of PS1 function, in isogenic human stem cells. *Cell Rep.* **5**, 974–985 (2013).
32. S. Veugelen, T. Saito, T. C. Saido, L. Chávez-Gutiérrez, B. De Strooper, Familial Alzheimer's disease mutations in Presenilin generate amyloidogenic Aβ peptide seeds. *Neuron* **90**, 410–416 (2016).
33. H. Watanabe, M. Iqbal, J. Zheng, M. Wines-Samuels, J. Shen, Partial loss of presenilin impairs age-dependent neuronal survival in the cerebral cortex. *J. Neurosci.* **34**, 15912–15922 (2014).
34. J. Kang, S. Shin, N. Perrimon, J. Shen, An evolutionarily conserved role of presenilin in neuronal protection in the aging *Drosophila* brain. *Genetics* **206**, 1479–1493 (2017).
35. J. Kang *et al.*, Lipophorin receptors genetically modulate neurodegeneration caused by reduction of Psn expression in the aging *Drosophila* brain. *Genetics* **226**, iyad202 (2024).
36. G. G. Glenner, C. W. Wong, Alzheimer's disease: Initial report of the purification and characterization of a novel cerebrovascular amyloid protein. *Biochem. Biophys. Res. Commun.* **120**, 885–890 (1984).

37. G. G. Glenner, C. W. Wong, Alzheimer's disease and Down's syndrome: Sharing of a unique cerebrovascular amyloid fibril protein. *Biochem. Biophys. Res. Commun.* **122**, 1131–1135 (1984).
38. R. D. Terry *et al.*, Physical basis of cognitive alterations in Alzheimer's disease: Synapse loss is the major correlate of cognitive impairment. *Ann. Neurol.* **30**, 572–580 (1991).
39. M. C. Irizarry, M. McNamara, K. Fedorchak, K. Hsiao, B. T. Hyman, APPSw transgenic mice develop age-related A beta deposits and neuropil abnormalities, but no neuronal loss in CA1. *J. Neuropathol. Exp. Neurol.* **56**, 965–973 (1997).
40. S. H. Lee *et al.*, APP family regulates neuronal excitability and synaptic plasticity but not neuronal survival. *Neuron* **108**, 676–690.e678 (2020).
41. X. C. Bai *et al.*, An atomic structure of human γ -secretase. *Nature* **525**, 212–217 (2015).
42. J. Cummings, G. Lee, A. Ritter, M. Sabbagh, K. Zhong, Alzheimer's disease drug development pipeline: 2020. *Alzheimers Dement.* **6**, e12050 (2020).
43. C. H. van Dyck *et al.*, Lecanemab in early Alzheimer's disease. *N. Engl. J. Med.* **388**, 9–21 (2023).
44. J. Kang, H. Watanabe, J. Shen, Protocols for assessing neurodegenerative phenotypes in Alzheimer's mouse models. *STAR Protocols* **2**, 100654 (2021).